

Article

Not peer-reviewed version

# Improving the Bio-Oil Quality of Residual Biomass Pyrolysis by Chemical Activation: Effect of Alkalis and Acid Pre-treatment

Gerson Valdez Daniel , Flávio Pinheiro Valois , Sammy Jonatan Bremer , Kelly Christina Alves Bezerra , Lauro Henrique Hamoy Guerreiro , [Marcelo Costa Santos](#) , Lucas Pinto Bernar , Waldeci Paraguassu Feio , Luiz Gabriel Santos Moreira , Neyson Martins Mendonça , [Douglas Alberto Rocha De Castro](#) , [Sergio Duvoisin Junior](#) , [Luiz Eduardo Pizarro Borges](#) , [Nélio Teixeira Machado](#) \*

Posted Date: 3 March 2023

doi: 10.20944/preprints202303.0052.v1

Keywords: Açaí seeds; Chemical activation; Pyrolysis; Acidity; Liquid hydrocarbons



Preprints.org is a free multidiscipline platform providing preprint service that is dedicated to making early versions of research outputs permanently available and citable. Preprints posted at Preprints.org appear in Web of Science, Crossref, Google Scholar, Scilit, Europe PMC.

Copyright: This is an open access article distributed under the Creative Commons Attribution License which permits unrestricted use, distribution, and reproduction in any medium, provided the original work is properly cited.

## Article

# Improving the Bio-Oil Quality of Residual Biomass Pyrolysis by Chemical Activation: Effect of Alkalis and Acid Pre-Treatment

Gérson Daniel Valdez <sup>1</sup>, Flávio Pinheiro Valois <sup>1</sup>, Sammy Jonatan Bremer <sup>2</sup>, Kelly Christina Alves Bezerra <sup>3</sup>, Lauro Henrique Hamoy Guerreiro <sup>4</sup>, Marcelo Costa Santos <sup>4</sup>, Lucas Pinto Bernar <sup>5</sup>, Waldeci Paraguassu Feio <sup>6</sup>, Luiz Gabriel Santos Moreira <sup>7</sup>, Neyson Martins Mendonça <sup>7</sup>, Douglas Alberto Rocha de Castro <sup>8</sup>, Sergio Duvoisin Jr. <sup>9</sup>, Luiz Eduardo Pizarro Borges <sup>10</sup> and Nélío Teixeira Machado <sup>1,3,4,6,\*</sup>

<sup>1</sup> Graduate Program of Sanitary and Environment Engineering, Campus Profissional-UFPA, Universidade Federal do Pará, Rua Corrêa N° 1, Belém 66075-900, Brazil

<sup>2</sup> Hochschule für Technik und Wirtschaft Berlin (HTW-Berlin), Wilhelminenhofstraße 75A, 12459 Berlin, Germany, Fachbereich 1, Energy und Informationen

<sup>3</sup> Graduate Program of Civil Engineering, Campus Profissional-UFPA, Universidade Federal do Pará, Rua Corrêa N° 1, Belém 66075-900, Brazil

<sup>4</sup> Graduate Program of Chemical Engineering, Campus Profissional-UFPA, Universidade Federal do Pará, Rua Corrêa N° 1, Belém 66075-900, Brazil

<sup>5</sup> Graduate Program of Natural Resources Engineering of Amazon, Campus Profissional-UFPA, Universidade Federal do Pará, Rua Augusto Corrêa N° 1, Belém 66075-110, Brazil

<sup>6</sup> Faculty of Physics, Campus Básico-UFPA, Universidade Federal do Pará, Rua Corrêa N° 1, Belém 66075-110, Brazil

<sup>7</sup> Faculty of Sanitary and Environmental Engineering, Campus Profissional-UFPA, Universidade Federal do Pará, Rua Corrêa N° 1, Belém 66075-900, Brazil

<sup>8</sup> Centro Universitário Luterano de Manaus – CEULM/ULBRA, Avenida Carlos Drummond de Andrade N°. 1460, Manaus 69077-730, Brazil

<sup>9</sup> Faculty of Chemical Engineering, Universidade do Estado do Amazonas-UEA, Avenida Darcy Vargas N°. 1200, Manaus 69050-020, Brazil

<sup>10</sup> Laboratory of Catalyst Preparation and Catalytic Cracking, Section of Chemical Engineering, Instituto Militar de Engenharia-IME, Praça General Tibúrcio N°. 80, Rio de Janeiro 22290-270, Brazil

\* Correspondence: machado@ufpa.br; Tel.: +55-91-984-620-325

**Abstract:** This work investigated the effect of temperature and acid or alkalis chemical activation by pyrolysis of Açaí seeds (*Euterpe Oleraceae*, Mart.) on the yield of bio-oil, hydrocarbon content of bio-oil, and chemical composition of aqueous phase. The experiments were carried out at 350, 400, and 450 °C and 1.0 atmosphere, KOH and HCl activation, in laboratory scale. The acidity of bio-oils and aqueous phases determined by AOCS methods, while the chemical composition of bio-oils and aqueous phase by GC-MS and FT-IR. The bio-char characterized by XRD. For the activation with KOH, the XRD analysis identified the presence of Kalicinite (KHCO<sub>3</sub>), the dominant crystalline phase in bio-char, while an amorphous phase was identified in bio-chars for the activation with HCl. The yield of bio-oil, for the pyrolysis of Açaí seeds activated with KOH, varied between 3.19 and 6.79 (wt.%), showing a smooth exponential increase with temperature. The acidity of bio-oil varied between 12.3 and 257.6 mgKOH/g, decreasing exponentially with temperature, while the acidity of aqueous phase lies between 17.9 and 118.9 mgKOH/g, showing and exponential decay behavior with temperature, demonstrating that higher temperatures favor not only the yield of bio-oil but also bio-oils with lower acidity. For the pyrolysis experiments activated with HCl, the yield of bio-oil varied between 2.13 and 3.37 (wt.%), decreasing linearly with temperature, while that of gas phase varied between 17.91 and 37.94 (wt.%), increasing linearly with temperature. The acidity of bio-oil varied between 127.1 and 218.5 mgKOH/g, increasing with temperature, showing that higher temperatures did not favor the yield of bio-oil and bio-oils acidity. For the chemical activation with KOH, the FT-IR analysis of bio-oils identified the presence of chemical groups characteristics of hydrocarbons and oxygenates, while that of aqueous phase only groups characteristics of

oxygenates. For the chemical activation with HCl, the FT-IR analysis of bio-oil and aqueous phases identified only the presence of groups characteristics of oxygenates. For the experiments with KOH activation, the GC-MS of bio-oil identified the presence of hydrocarbons (alkanes, alkenes, cycloalkanes, cycloalkenes, and aromatics) and oxygenates (carboxylic acids, phenols, ketones, and esters). The concentration of hydrocarbons varied between 10.19 to 25.71 (area.%), increasing with temperature, while that of oxygenates from 52.69 to 72.15 (area.%), decreasing with temperature. For the experiments with HCl activation, the GC-MS of bio-oil identified only the presence of oxygenates. Finally, it can be concluded that chemical activation of Açaí seeds with KOH favors the not only the yield of bio-oil but also the content of hydrocarbons while activation with HCl produced bio-oils with only oxygen compounds.

**Keywords:** Açaí seeds; chemical activation; pyrolysis; acidity; liquid hydrocarbons

---

## 1. Introduction

The population growth and increasing waste generation in low, medium and high income lands poses a huge challenge concerning the waste management and its final destination [1,2]. Lignin-cellulosic based biomass is class of waste to be considered, due to its volume generated, particularly those associated to agricultural activities [3].

Açaí (*Euterpe oleracea*, Mart.), a palm of native occurrence in the floodplains of the Amazon [4–6], has great economic importance not only for the agroindustry, but also for rural communities whose economic income is based on *extractive activities* in the state of Pará-Brazil [7]. The pulp of Açaí (*Euterpe oleracea*, Mart.) fruits *in nature* is processed with warm H<sub>2</sub>O to produce a thick, purple juice [3,6], generating a residue [1,2], the seeds.

The seeds of Açaí (*Euterpe oleracea*, Mart.), a rich lignin-cellulosic biomass, have great potential for energy and fuels [8–12]. In the 2017 crop year, around 1200-1274 million tons of Açaí fruits were produced in Brazil, and the state of Pará the main producer in Brazil (94%), generating a large amount of solid waste [7,13].

Pyrolysis is a thermo-chemical process with great potential to convert biomass into energy & fuels [8,11]. The reaction products include a gas, a liquid (bio-oil) and a solid (bio-char) [8,11]. The yield and properties of reaction products is a function of biomass characteristics, type of pyrolysis process, type of reactors, operating mode, and process parameters, particularly, the temperature, type of catalyst, and catalyst-to-biomass ratio [14–16].

In the last years, studies on the pyrolysis of residual Açaí seeds [8,11,17–29], most of them aiming to produce a carbonaceous solid with activated carbon characteristics, were reported in the literature [8,17–29].

Despite studies on the pyrolysis of residual Açaí seeds *in nature* [17–19], and activated residual Açaí seeds [8,20–29], until the moment, no systematic study has investigated the effect of acid and alkalis activation of residual Açaí seeds on the yield, chemical composition and acidity of bio-oil and aqueous phase.

This work aims to investigate the effect of temperature and acid (HCl) and alkalis (KOH) chemical activation of residual Açaí seeds on the yield, hydrocarbon content and acidity of bio-oil, as well as on the chemical composition and acidity of aqueous phase by pyrolysis of residual Açaí seeds at 350, 400, and 450 °C and 1.0 atmosphere, activated with aqueous solutions of 2.0 M KOH and HCl, in laboratory scale.

## 2. Materials and Methods

### 2.1. Methodology

The process flow sheet shown in Figure 1 summarizes the applied methodology, described in a logical sequence of ideas, chemical methods, and procedures to produce bio-oil by pyrolysis of Açaí

seeds at 350, 400, and 450 °C, 1.0 atm, activated with 2.0 M KOH and HCl, using a fixed bed reactor, in laboratory scale. Initially, the Açaí seeds, discharged/disposed on the sidewalks and streets, after the processing of Açaí fruits *in nature*, are collected. Afterwards, it is subjected to pre-treatment drying, milling, and sieving. The powder biomass is chemically activated with KOH and HCl, followed by H<sub>2</sub>O washing and drying. The experiments were carried out using a process schema consisting of a pyrolysis reactor coupled to condenser without catalyst. The effect of acid and alkalis activation analyzed. The physical-chemistry properties and chemical composition of bio-oil and aqueous phase determined.

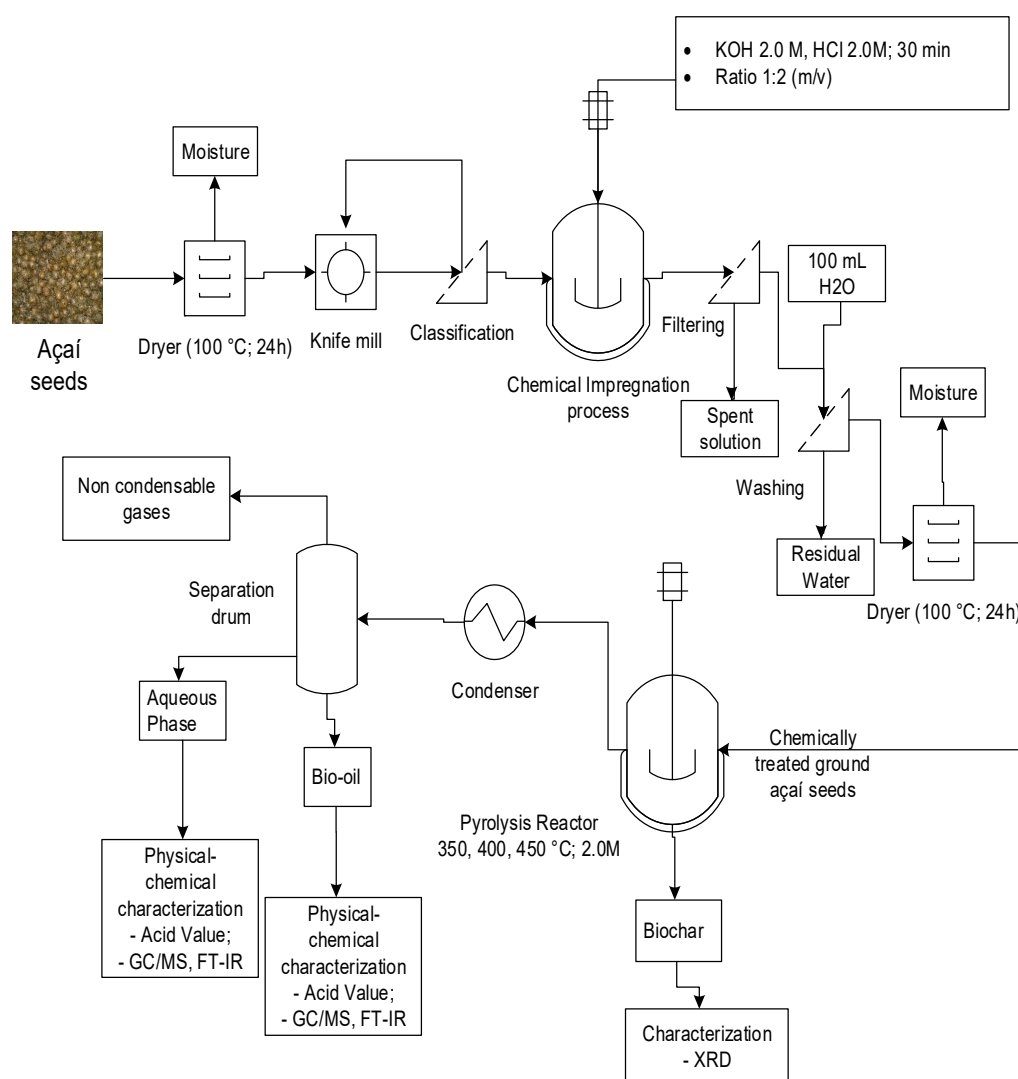


**Figure 1.** Process flow schema of bio-oil production by pyrolysis of Açaí seeds at 350, 400, and 450 °C, 1.0 atm, activated with 2.0 M KOH and HCl, using a fixed bed reactor, in laboratory scale.

## 2.2. Materials

The seeds of Açaí (*Euterpe oleracea* Mart.), discharged/disposed on the sidewalks and streets by a small store of Açaí commercialization, located in the District of Jurunas, Belém-Pará-Brazil, were collected and conditioned in plastic bags. Figure 2 shows seeds of Açaí (*Euterpe oleracea*, Mart.) discharged on the sidewalks and streets by a small store of Açaí commercialization, located in the District of Jurunas, Belém-Pará-Brazil.





**Figure 2.** Seeds of Açaí (*Euterpe oleracea*, Mart.) discharged on the sidewalks and streets by a small store of Açaí commercialization, located in the District of Jurunas, Belém-Pará-Brazil.

### 2.3. Pre-treatment of Açaí seeds (*Euterpe oleracea*, Mart.)

The Seeds of Açaí (*Euterpe oleracea*, Mart.) were submitted to physical pre-treatment drying, grinding, and sieving. Afterwards, the dried, grinded and sieved seeds were activated chemically using solutions of 2.0 M KOH and 2.0 M HCl, and the procedures described in detail in sections 2.3.1 and 2.3.2.

#### 2.3.1. Physical pre-treatment of Açaí seeds (*Euterpe oleracea*, Mart.)

The seeds of Açaí (*Euterpe oleracea*, Mart.) were dried at 105°C for 24 hours using an analogic controlled oven (DeLeo, Porto Alegre-Brazil, Model: DL-SE). Afterward, the dried seeds were grinded using a laboratory knife cutting mill (TRAPP, Brazil, Model: TRF 600). Then, the dried and grinded Açaí seeds were sieved using a set of sieves of 28, 35, 48, 60 Mesh in order to remove the excess fiber material, as well as to decrease the specific particle diameter. A charge of Açaí (*Euterpe oleracea*, Mart.) seeds *in nature* weighting approximately 5.0 kg was collected for the pyrolysis experiments. The drying, grinding and sieving of Açaí seeds is shown in Figure 3.



**Figure 3.** Açaí seeds after drying, milling, and sieving process [Dried Açaí seeds (a); Knife cutting mill (b); Mechanical sieve shaker (c); Dried, grinded and sieved Açaí seeds (d)].

### 2.3.2. Chemical activation of Açaí seeds (*Euterpe oleracea*, Mart.)

After the physical pre-treatment described in section 2.3.1, the dried, grinded and sieved Açaí seeds were activated chemically with 2.0 M KOH or 2.0 M HCl solutions and the procedures described as follows: Approximately 120 g of dried, ground, and sieved Açaí seeds was mixed manually with 240 mL of a 2.0 M HCl solution or 240 mL of a 2.0 M KOH (1:2 mass/volume ratio) for 30 minutes, using a Becker of 500 mL. The addition of 2.0 M HCl or 2.0 M KOH solutions into the fine powder of Açaí seeds produced a moisture sludge. Afterwards, the moist sludge was placed into a paper filter and washed with 100 mL distilled water for 24 hours, as described elsewhere [9]. Then, the retained moist sludge is submitted to drying at  $100\text{ }^{\circ}\text{C} \pm 5\text{ }^{\circ}\text{C}$  for 24 hours, using an analogic controlled oven (DeLeo, Porto Alegre-Brazil, Model: DL-SE). Figure 4 shows the chemical activation of Açaí seeds fine powders with a 2.0 M KOH solution.



**Figure 4.** Chemical activation of dried, grinded and sieved Açaí seeds with 2.0 M KOH solution [Açaí seeds fine powders mixed with 2.0 M KOH solution (a); washing/filtration of Açaí paste cake (b); KOH activated Açaí fine powders seeds (c)].

### 2.4. Centesimal and immediate characterization of Açaí seeds

The Açaí seeds (*Euterpe oleracea*, Mart.) were previously characterized for moisture, ash, volatiles, and fixed carbon [9,11], as well as for lipids, proteins, fibers, cellulose, hemicellulose, and insoluble lignin [30].

### 2.5. Experimental apparatus and procedures

#### 2.5.1. Experimental apparatus

Figure 5 illustrates the laboratory scale borosilicate glass reactor. The experimental unit consists of a cylindrical borosilicate glass reactor of 3.3 cm internal diameter and 22.8 height ( $V_{\text{Reactor}} = 195\text{ mL}$ ), a Liebig glass condenser, a ceramic heating system of 800 W, a glass separating funnel with a gas outlet at the top, and a digital temperature control, as described in detail elsewhere [8,11,31–33]. The glass borosilicate reactor is inserted inside a cylindrical oven with a ceramic resistance of 800 W. The digital temperature controller (THERMA, São Paulo-Brazil, Model: TH90DP202-000), makes it possible to control the temperature and the heating rate. The temperature inside the reactor was measured with a K-type thermocouple (Ecil, São Paulo-Brazil, Model: QK. 2). A Liebig condenser, using cooling  $\text{H}_2\text{O}$  supplied by a digital thermostatic recirculation bath, is connected to the exit of glass reactor using a Y shaped connection. The liquid phase products were collected inside a 50 mL borosilicate glass flask. The non-condensable gases (e.g.,  $\text{CH}_4$ ,  $\text{C}_2\text{H}_6$ ,  $\text{C}_3\text{H}_8$ ,  $\text{O}_2$ ,  $\text{CO}_2$ , etc.) flow through an opening in the  $90^\circ$  curve, coupled between the Liebig condenser and the glass separating funnel, to the flare system.



**Figure 5.** Laboratory scale borosilicate glass pyrolysis reactor.

### 2.5.2. Experimental procedures

By the pyrolysis of chemically activated Açaí seeds, approximately 40.0 g weighed using a semi-analytical balance (Marte Científica e Instrumentação Industrial Ltda, São-Paulo-Brazil, Model: AD330). Then, the chemically activated Açaí seeds placed inside the glass reactor. After connecting the glass reactor to the Liebig condenser, using a Y shaped connection, and the condenser to the separating funnel, the cooling system is turned on and the water temperature was set at 10 °C. Then, the desired heating rate (10 °C/min), and temperature (350, 400, or 450 °C) were set-up. The reactor temperature was recorded every 10-15 minutes. The mass of liquid phase (bio-oil + aqueous phase) and biochar (coke) were collected and weighed, and the mass of gas computed by difference. The bio-oil was separated from aqueous phase by decantation inside the separation funnel. Afterwards, the bio-oil physicochemical characterized for acid value.

### 2.6. Physical-chemistry analysis and chemical composition of bio-oils and aqueous phase

#### 2.6.1. Physical-chemistry analysis of bio-oils and aqueous phase

The bio-oils and aqueous phases were physicochemical analyzed for acid value according to official methods (AOCS Cd 3d-63), as described elsewhere [31–34].

#### 2.6.2. Chemical composition of bio-oils and aqueous phase

##### 2.6.2.1. GC-MS analysis

The chemical composition of bio-oils and aqueous phases obtained by pyrolysis at 350, 400, and 450 °C and 1.0 atmosphere, and 450 °C and 1.0 atmosphere, with 2.0 M KOH and HCl, in laboratory scale, determined by GC-MS and the equipment and procedures described in detail in the literature by Castro *et. al.* [8,11,15,16,35–38]. The peak intensity, retention times, and compounds identification were analyzed according to the NIST mass spectra library. The concentrations were expressed in area, as no internal standard was injected to compare the peak areas.

##### 2.6.2.2. FT-IR analysis

The identification of chemical groups (carbonyl, carboxyl, hydroxyl, phenyl, etc.) preset in bio-oils aqueous phase obtained by pyrolysis at 350, 400, and 450 °C and 1.0 atmosphere, and 450 °C and



1.0 atmosphere, with 2.0 M KOH and HCl, in laboratory scale, performed by Fourier transform infrared spectroscopy (FT-IR) using a spectrometer (BRUKER, Ettlingen-Germany, Model: VERTEX 70v) at the Laboratory of vibrational spectroscopy and high pressure (LEVAP-PPGF/UFGPA). The identification of characteristics chemical groups performed as described in the literature [11,31–34].

## 2.7. Characterization of hidrochar

### 2.7.1. XRD analysis

The crystalline and/or mineralogical characterization of bio-char obtained by pyrolysis of chemically activated Açaí seeds with 2.0 M KOH and 2.0 M HCl solutions, at 350, 400, and 450 °C and 1.0 atmosphere, in laboratory scale, performed by x-ray diffraction using a diffractometer (Rigaku, Japan, Model: MiniFlex600) at the Laboratory of Structural Characterization (FEMAT/UNIFESSPA) and the equipment specifications described as follows: *generator* (maximum power: 600 W; tube voltage: 40 kV; tube current: 15 mA; X-ray tube: Cu), *optics* (fixed divergence, scattering and receiving slit; filter; K $\beta$  sheet; monochromator: graphite; soller slit: 5.0°), *goniometer* (model: vertical, radius: 150 mm, scanning range: -3 A , 145° (2 $\theta$ ); scanning speed: 0.01 to 100°/min (2 $\theta$ ); accuracy:  $\pm$  0.02°) and *detector* (high-speed silicone tape). The identification of crystalline and/or amorphous carbonaceous phases present in bio-char performed as described in the literature [9,15,16,39,40].

## 2.8. Mass balances by pyrolysis of Açaí seeds

Application of an overall mass balance inside the pyrolysis glass reactor, operating in batch mode, closed thermodynamic system, yields the following equations for the pyrolysis reactor.

$$m_{in,pyrolysis} - m_{out,pyrolysis} = 0 \quad (1)$$

$$m_{in,pyrolysis} = 0 \quad (2)$$

$$-m_{out,pyrolysis} = m_{vapors,pyrolysis} \quad (3)$$

Where  $m_{in,pyrolysis}$  is the mass flow rate entering the glass reactor,  $m_{out,pyrolysis}$  is the mass flow rate leaving the glass reactor,  $m_{vapors,pyrolysis}$  is the mass flow rate of pyrolysis vapors/volatiles leaving the glass reactor. Assuming that all the vapors/volatiles leaving glass reactor splits into bio-oil, aqueous phase, and non-condensable gases, the following equations applies.

$$m_{vapors,pyrolysis} = \frac{dm_{vapors}}{d\tau} \quad (4)$$

$$\frac{dm_{vapors}}{d\tau} = 0 \quad (5)$$

$$m_{vapors,pyrolysis} = m_{gas} + m_{aqueous\ phase} + m_{bio-oil} \quad (6)$$

Where  $m_{gas}$  is the mass flow rate of non-condensable gases leaving the glass reactor, computed by difference, and  $m_{bio-oil}$  is the mass flow rate of bio-oil leaving the condenser, and  $m_{aqueous\ phase}$  is the mass flow rate of aqueous phase leaving the condenser. The mass of solid remaining inside the glass reactor is  $m_{solid}$ . By performing a steady state global mass balance within the glass reactor yields equation (7).

$$m_{Feed} = m_{solid} + m_{gas} + m_{bio-oil} + m_{aqueous\ phase} \quad (7)$$

The process performance evaluated by computing the yields of bio-oil, aqueous phase, and solid (coke) defined by equations (8), (9) and (10), respectively, and the yield of gas by difference, using equation (11).

$$Y_{bio-oil}[\%] = \frac{M_{Bio-oil}}{M_{Feed}} \times 100 \quad (8)$$



$$Y_{Aqueous\ phase}[\%] = \frac{M_{Aqueous\ phase}}{M_{Feed}} \times 100 \quad (9)$$

$$Y_{Solids}[\%] = \frac{M_{Solids}}{M_{Feed}} \times 100 \quad (10)$$

$$Y_{gas}[\%] = 100 - (Y_{bio-oil} + Y_{Solids} + Y_{Aqueous\ phase}) \quad (11)$$

## 4. Results

### 4.1. Characterization of bio-char

#### 4.1.1. XRD analysis

##### 4.1.1.1. Effect of KOH activation

The XRD of bio-char produced by pyrolysis of Açaí seeds at 350, 400, and 450 °C, 1.0 atmosphere, activated with 2.0 M KOH, in laboratory scale, is shown in Figure 6 [350 °C (a); 400 °C (b); 450 °C (c)], and the analysis of peaks characteristics (Intensity, Position: 2θ, Percentage: %) of crystalline phases identified by XRD in bio-chars by pyrolysis of Açaí seeds (*Euterpe Oleracea*, Mart), activated with 2.0 M KOH solution, at 350, 400, and 450 °C, 1.0 atmosphere, illustrated in Table 1. The diffractogram of bio-chars illustrated in Figure 7 identified peaks of medium and high intensity associated to Kalicinite (KHCO<sub>3</sub>), the dominant crystalline phase in bio-char. This is according to the results of Prakongkep *et. al.* [40], who investigated the chemical properties (pH, conductivity, and ash), elemental analysis (C, N), micro and macro nutrients (Si, Al, Ca, Mg, Na, K, P, S, Fe, Mn, As), as well as morphological (SEM) and crystalline (XRD) characterization of biochar produced by pyrolysis of durian shell at 350 °C, in laboratory scale. Prakongkep *et. al.* [40], reported that Kalicinite (KHCO<sub>3</sub>) was the dominant crystalline phase in bio-char. Moreover, Han Lee *et. al.* [41], studied XRD patterns of chemically modified biochar by K agents and found similar behavior, showing striking similarity to the diffractograms of biochar illustrated in Figure 6. Díaz-Terán *et. al.* [42], studied the chemical activation of lignocellulosic material with KOH and XRD patterns revealed the presence of KHCO<sub>3</sub> (Kalicinite) and K<sub>2</sub>CO<sub>3</sub> crystalline, demonstrating that peak intensity increases with temperature, as confirmed in Table 1.

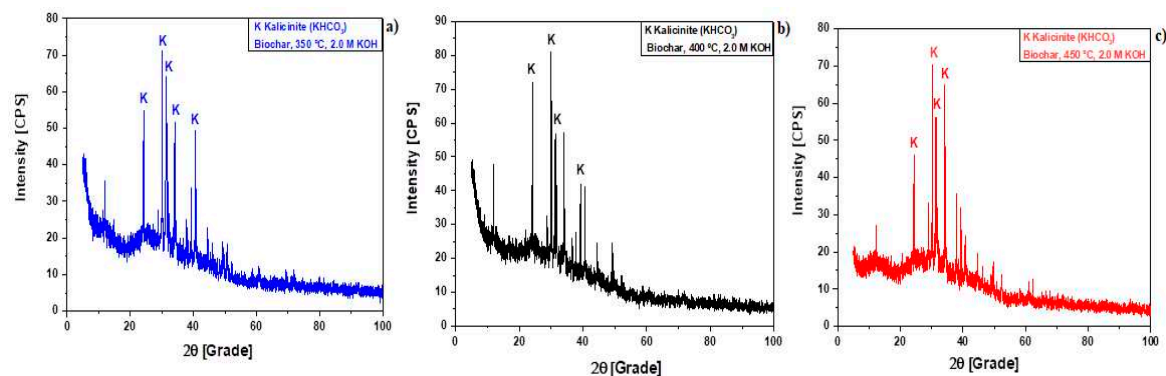


**Figure 6.** XRD of biochar produced by pyrolysis of Açaí seeds at 350 , 400, and 450 °C, 1.0 atm, activated with 2.0 M KOH, in laboratory scale [350 °C (a); 400 °C (b); 450 °C (c)].

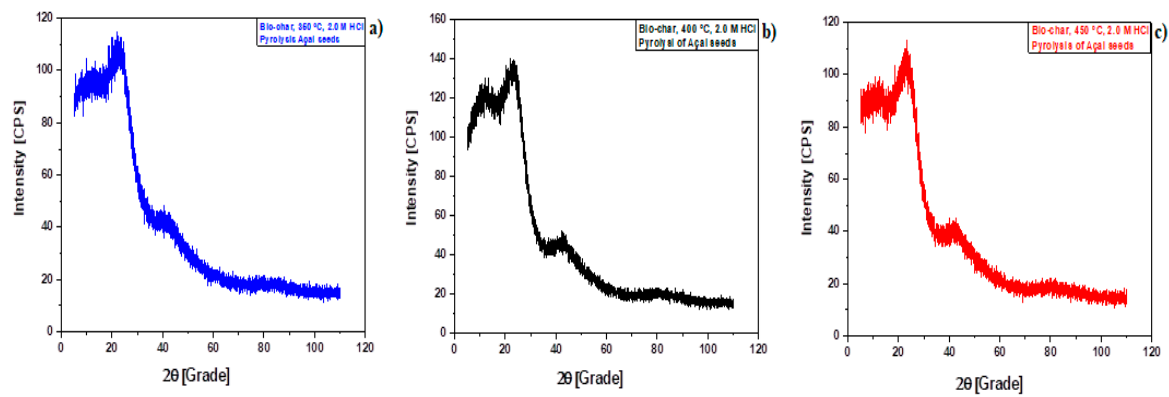


**Figure 7.** XRD of bio-char produced by pyrolysis of Açai seeds at 350 , 400, and 450 °C, 1.0 atm, activated with 2.0 M HCl, in laboratory scale [350 °C (a); 400 °C (b); 450 °C (c)].

**Table 1.** Analysis of peaks characteristics (Intensity, Position: 2θ, Percentage: %) of crystalline phases identified by XRD in bio-chars by pyrolysis of Açai seeds (*Euterpe Oleracea*, Mart), activated with 2.0 M KOH solution, at 350, 400, and 450 °C, 1.0 atmosphere, using a borosilicate glass reactor, in laboratory scale.

Temperature	Peaks Intensity, Position (2θ), and Percentage (%)					
	Medium		Medium		High	
	2θ	(%)	2θ	(%)	2θ	(%)
350 °C	24.2	66.8	40.6	68.6	30.0	100
400 °C	Medium		High		High	
	2θ	(%)	2θ	(%)	2θ	(%)
	31.3	62.2	24.1	81.73	30.0	100
450 °C	High		High		High	
	2θ	(%)	2θ	(%)	2θ	(%)
	30.2	100.0	31.3	79.9	34.2	92.1

4.1.1.2. Effect of HCl activation

The XRD of bio-char produced by pyrolysis of Açai seeds at 350, 400, and 450 °C, 1.0 atmosphere, activated with 2.0 M HCl, in laboratory scale, is shown in Figure 7 [350 °C (a); 400 °C (b); 450 °C (c)]. In fact, the pre-treatment of Açai seeds *in nature* with HCl, a strong Arrhenius acid, leachates all the inorganic compounds present within the biomass, so that pyrolysis of de-mineralized Açai seeds at 350, 400, and 450 °C, 1.0 atmosphere, produces a solid phase (bio-char) containing significant amount of highly disordered material, *amorphous carbon*, responsible for the *back ground intensity of the diffractograms* [39], as illustrated in Figure 7. This is according to the results presented by *Manoj and Kunjomana* [39], who study the X-ray diffraction of de-mineralized coal with HF, a strong Arrhenius acid, showing *back ground intensity in the diffractograms* due to significant amount of amorphous carbon.

4.2. Pyrolysis of activated açai seeds (*Euterpe Oleracea*, Mart.)

4.2.1. Process conditions, mass balances, and yields of reaction products by pyrolysis of activated Açai seeds (*Euterpe Oleracea*, Mart.) with KOH

Table 2 illustrates the process parameters, mass balances, yields of reaction products (liquids, solids, H<sub>2</sub>O, and gas), and acidity of bio-oils by pyrolysis of activated Açai seeds at 350, 400, and 450 °C, 1.0 atm, activated with 2.0 M KOH, using a borosilicate glass reactor, in laboratory scale.

**Table 2.** Process parameters, mass balances, yields of reaction products (liquids, solids, H<sub>2</sub>O, and gas), and acidity of bio-oils by pyrolysis of Açaí seeds (*Euterpe Oleracea*, Mart), activated with 2.0 M KOH solution, at 350, 400, and 450 °C, 1.0 atmosphere, using a borosilicate glass reactor, in laboratory scale.

Process Parameters	2.0 M KOH		
	350 °C	400 °C	450 °C
Mass of Açaí seeds (g)	40.12	40.12	40.06
Cracking time (min)	72	72	72
Yield of Bio-oil (wt.%)	3.19	6.58	6.79
Yield of H <sub>2</sub> O (wt.%)	20.34	25.57	20.99
Yield of Hydro-char (wt.%)	43.37	33.40	40.36
Yield of Gas (wt.%)	33.10	34.45	31.85
Acidity (mg KOH/g)	257.6	15.0	12.3

The pyrolysis experiments of activated Açaí seeds at 350, 400, and 450 °C, 1.0 atm, activated with 2.0 M KOH, using a borosilicate glass reactor, in laboratory scale, show yields of bio-oil between 3.19 and 6.79% (wt.), aqueous phase yields between 20.34 and 25.57% (wt.), hydro-char yields between 33.40 and 43.37% (wt.), and yields of gas between 31.85 and 34.45% (wt.). The yields of bio-oil are similar to those reported by Serrão *et. al.* [43], who studied the pyrolysis of Açaí seeds *in nature* at 350, 400, and 450 °C, 1.0 atmosphere, in pilot scale, showing yields between 2.0 and 4.39% (wt.), as well as those reported by Castro *et. al.* [11], who studied the pyrolysis of Açaí seeds *in nature* at 450 °C, 1.0 atmosphere, in pilot, bench, and laboratory scale, showing bio-oil yields of 4.37, 6.60, and 13.09% (wt.), respectively. In addition, the experimental data for biochar yields illustrated in Table 2 is according to similar data reported for the pyrolysis of Açaí seeds reported in the literature [9,11,18–20,22], showing biochar yields between 27.0 and 49.0% (wt.) for the pyrolysis of Açaí seeds *in nature* [9,18–20], and biochar yields between 26.44 and 72.50% (wt.) for the pyrolysis of Açaí seeds chemically activated [11,22].

The yields of reaction products (liquids, solids, H<sub>2</sub>O, and gas) by pyrolysis of activated Açaí seeds at 350, 400, and 450 °C, 1.0 atm, activated with 2.0 M KOH, using a borosilicate glass reactor, in laboratory scale, are shown in Figure 8. The yield of bio-oil shows a smooth increase with temperature, and was correlated with a first order exponential decay model, exhibiting root-mean-square error (*r*<sup>2</sup>) of 1.00. The results are according to those reported by Serrão *et. al.* [43], who investigated the pyrolysis of Açaí seeds *in nature* at 350, 400, and 450 °C, 1.0 atmosphere, in pilot scale, showing an increase of bio-oil yield with temperature. Moreover, the results are in agreement with similar studies for the yield of bio-oil by the pyrolysis of biomass reported in the literature [44–55], whereas the yield of bio-oil increases between 200 and 450 °C [44–55].

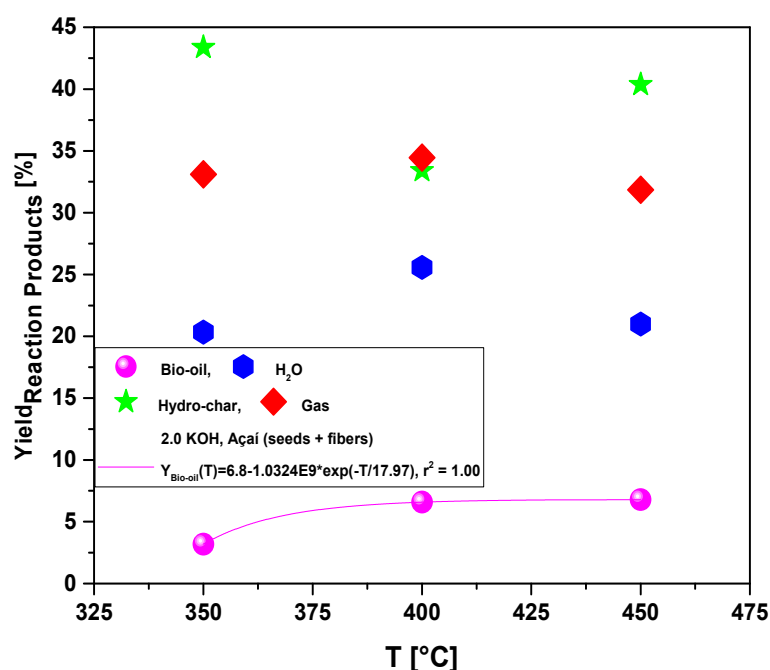


**Figure 8.** Yield of reaction products (bio-oil, H<sub>2</sub>O, hydro-char, gas) by pyrolysis of Açai seeds (*Euterpe Oleracea*, Mart), activated with 2.0 M KOH solution, at 350, 400, and 450 °C, 1.0 atmosphere, in laboratory scale.

#### 4.2.1.1. Effect of temperature on the composition of hydrocarbons and oxygenates in bio-oil

The effect of process temperature on the composition of hydrocarbons and oxygenates in bio-oil obtained by pyrolysis of Açai seeds (*Euterpe Oleracea*, Mart), activated with 2.0 M KOH solution, at 350, 400, and 450 °C, 1.0 atmosphere, in laboratory scale, is shown in Figure 9. The chemical functions (alkanes, alkenes, cycloalkanes, cycloalkenes, aromatics, esters, carboxylic acids, furans, phenols, aldehydes, alcohols, and ketones), sum of peak areas, CAS numbers, and retention times of all the molecules identified in bio-oil by GC-MS by pyrolysis of Açai seeds (*Euterpe Oleracea*, Mart), activated with 2.0 M KOH solution, at 350, 400, and 450 °C, 1.0 atmosphere, in laboratory scale, are illustrated in Supplementary Tables S1-S3. By increasing the temperature, the concentration of hydrocarbons increases, while that of oxygenates decreases. The concentrations of hydrocarbons were correlated with a first order exponential growth model, exhibiting root-mean-square error ( $r^2$ ) of 1.00, showing that higher pyrolysis temperatures favor the formation of hydrocarbons. The results are according to those reported by de Sousa *et al.* [56], who investigated the effect of process temperature on the concentration of hydrocarbons and oxygenates in bio-oil by the pyrolysis of Açai seeds *in nature* at 350, 400, and 450 °C, 1.0 atmosphere, in pilot scale. According to de Sousa *et al.* [56], the concentration of hydrocarbons increases, while that of oxygenates decreases with increasing temperature. According to de Sousa *et al.* [56], the concentration of oxygenates decrease with increasing temperature, showing that higher pyrolysis temperatures do not favor the formation of oxygenates [56]. The concentration of oxygenates in bio-oil were correlated with a first order exponential decay model, exhibiting in all the cases root-mean-square error ( $r^2$ ) of 1.00.



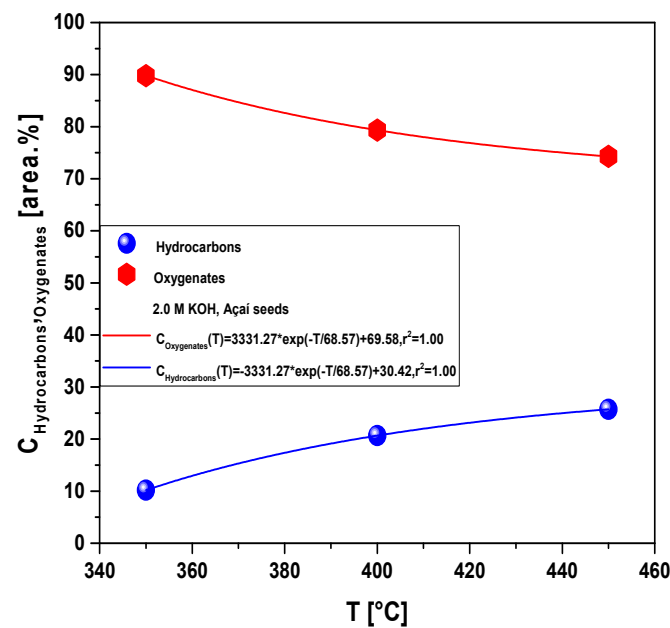


**Figure 9.** Concentration of hydrocarbons and oxygenates in bio-oil by pyrolysis of Açai seeds (*Euterpe Oleracea*, Mart), activated with 2.0 M KOH solution, at 350, 400, and 450 °C, 1.0 atmosphere, in laboratory scale.

The acid value (acidity) of bio-oils obtained by pyrolysis of Açai seeds (*Euterpe Oleracea*, Mart), activated with 2.0 M KOH solution, at 350, 400, and 450 °C, 1.0 atmosphere, in laboratory scale, is shown in Figure 10. The acidity of bio-oil decreases with increasing pyrolysis temperature, showing a sharp exponential decay behavior. The acidity of bio-oil varied between 257.6 and 12.3 (mgKOH/g) and correlated with a first order exponential decay model, exhibiting root-mean-square error ( $r^2$ ) of 1.00, corroborating with the results presented in Figure 9, that is, the higher the concentration of oxygenates in bio-oil, the higher the acidity of bio-oil.

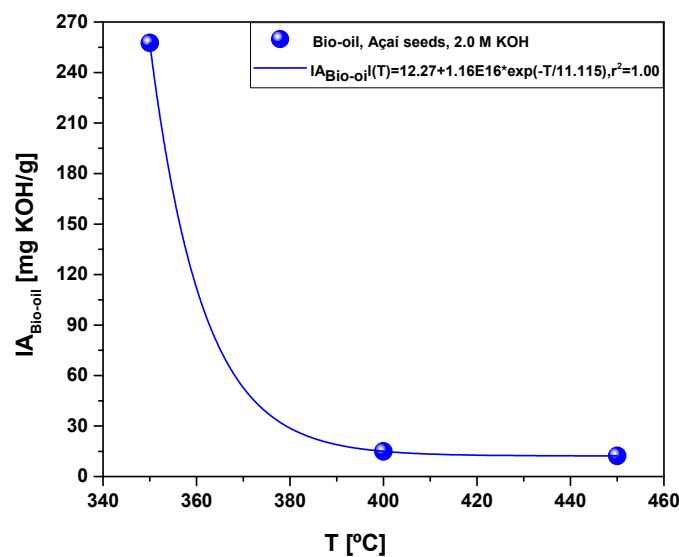


**Figure 10.** Acidity of bio-oil obtained by pyrolysis of Açai seeds (*Euterpe Oleracea*, Mart), activated with 2.0 M KOH solution, at 350, 400, and 450 °C, 1.0 atmosphere, in laboratory scale.

The chemical functions characteristics of hydrocarbons and oxygenates identified by FT-IR analysis of bio-oils obtained by pyrolysis of Açai seeds (*Euterpe Oleracea*, Mart), activated with 2.0 M KOH solution, at 350, 400, and 450 °C, 1.0 atmosphere, in laboratory scale, illustrated in Figure 11. The FT-IR identified adsorption bands characteristic of chemical functions/chemical bonds as shown in Table 3, confirming the presence of aliphatic hydrocarbons, carboxylic acids, alcohols, as well as the presence of H<sub>2</sub>O in bio-oils, being according to similar analysis described elsewhere [11,31–34,57,58].

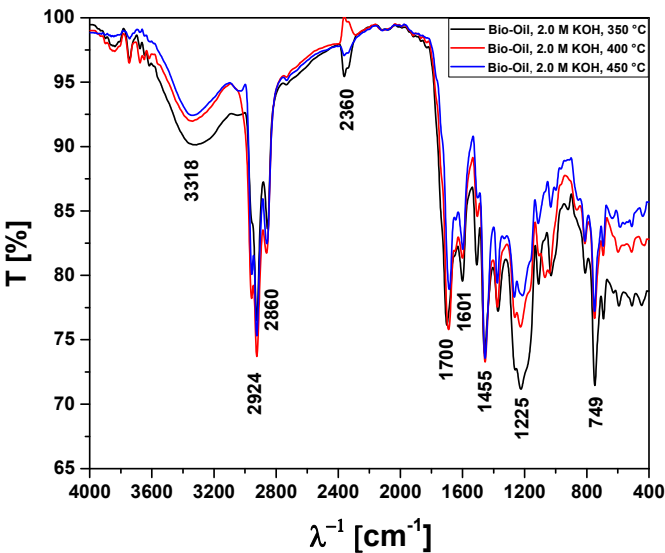


**Figure 11.** FT-IR analysis of bio-oils obtained by pyrolysis of Açai seeds (*Euterpe Oleracea*, Mart), activated with 2.0 M KOH solution, at 350, 400, and 450 °C, 1.0 atmosphere, in laboratory scale.

**Table 3.** Absorption bands and chemical functions/groups identified by FT-IR analysis of bio-oils obtained by pyrolysis of Açai seeds (*Euterpe Oleracea*, Mart), activated with 2.0 M KOH solution, at 350, 400, and 450 °C, 1.0 atmosphere, in laboratory scale.

Absorption Bands	Chemical Functions/Chemical Bonds
3400-3200 cm <sup>-1</sup>	ν-OH, hydrogen bonds of alcohol and H <sub>2</sub> O.
2870-2840 cm <sup>-1</sup>	ν <sub>s</sub> -CH <sub>2</sub> , methylene group CH <sub>2</sub> .
2930-2920 cm <sup>-1</sup>	ν <sub>as</sub> -CH <sub>2</sub> , methylene group CH <sub>2</sub> .
1709 cm <sup>-1</sup>	ν-C=O, carbonyl group of carboxylic acids and ketones.
1601 cm <sup>-1</sup>	νC=C-C, C=C-C ring-related stretching associated to phenols.
1465-1440 cm <sup>-1</sup>	δ <sub>as</sub> CH <sub>3</sub> , methyl group (C-H).
1200-1125 cm <sup>-1</sup>	ν-C-O, saturated alcohols (C-O).
1000-650 cm <sup>-1</sup>	γ =C-H, Alkenes (=C-H).

4.2.1.2. Effect of temperature on the composition of hydrocarbons and oxygenates in the aqueous phase

The chemical composition and acidity of aqueous phase, formed after pyrolysis of Açai seeds (*Euterpe Oleracea*, Mart), activated with 2.0 M KOH solution, at 350, 400, and 450 °C, 1.0 atmosphere, in laboratory scale, was determined by GC-MS, as illustrated in Table 4.

**Table 4.** Chemical composition and acidity (alcohols, carboxylic acids, ketones, phenols, and other oxygenates) of aqueous phase obtained by pyrolysis of Açaí seeds (*Euterpe Oleracea*, Mart), activated with 2.0 M KOH solution, at 350, 400, and 450 °C, 1.0 atmosphere, in laboratory scale, identified by GC-MS.

Chemical Composition $C_i$ (area.%)	2.0 M KOH		
	350 °C	400 °C	450 °C
Alcohols	2.34	20.74	26.62
Carboxylic Acids	<b>4.05</b>	<b>15.02</b>	<b>9.23</b>
Ketones	52.81	44.38	19.69
Oxygenates	40.80	19.86	44.46
$\sum_i^n C_i$	<b>100.00</b>	<b>100.00</b>	<b>100.00</b>
Acidity (mg KOH/g)	118.9	26.8	17.9

The chemical functions, sum of peak areas, CAS numbers, and retention times of compounds identified in aqueous phase by GC-MS analysis after pyrolysis of Açaí seeds (*Euterpe Oleracea*, Mart), activated with 2.0 M KOH solution, at 350, 400, and 450 °C, 1.0 atmosphere, in laboratory scale, are illustrated in Supplementary Tables S4–S6. The major oxygenates compounds identified in the aqueous phase were alcohols, carboxylic acids, and ketones. The remaining oxygen compounds summed and named *oxygenates* (*phenols, aldehydes, amines, etc.*). The composition of aqueous phase is according to similar studies reported in the literature [59–61]. Zhang *et al.* [59], identified the presence of carboxylic acids, ketones, phenols, and furans in the aqueous phase produced by pyrolysis of sawdust. Torri and Fabbri [60], investigated the chemical composition of aqueous phase by pyrolysis of corn stalk, identifying the presence of carboxylic acids, aldehydes, phenols, furans, sugars and N-compounds. Zhou *et al.* [61], reported the presence of carboxylic acids, aldehydes, phenols, ketones, furans, and furfurals sugars and amines on the composition of aqueous phase by pyrolysis of corn Stover.

Based on the fact that alcohols are weak acids, it's contribution to the acidity of aqueous phase is small or negligible. On the contrary, the  $\alpha$ -hydrogen atoms of ketones are acidic in nature, thus contributing to the acidity of aqueous phase. Finally, low carbon chain length carboxylic acids present in the aqueous phase have a great contribution to the acidity. As the concentration of ketones in the aqueous phase decreases, it is to be expected that acidity of aqueous phase to diminish, as shown in Figure 12. The acidity of aqueous correlated with a first order exponential decay model, exhibiting root-mean-square error ( $r^2$ ) of 1.00.

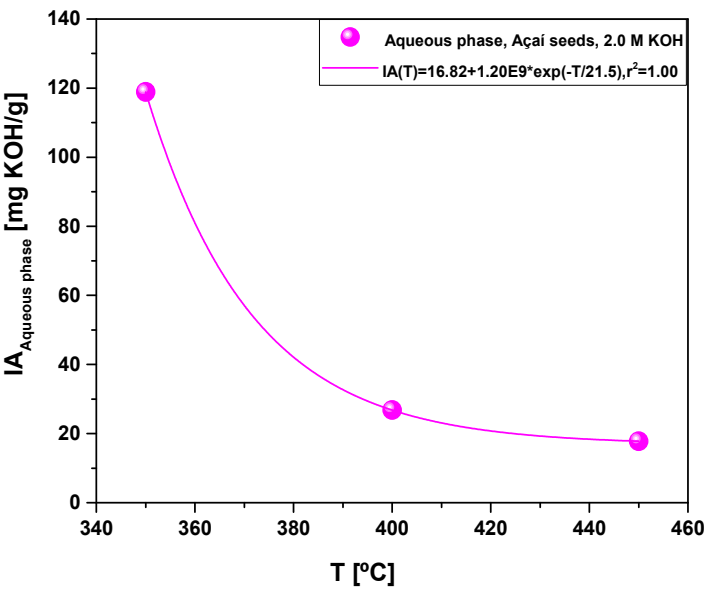


**Figure 12.** Acidity of aqueous phase obtained by pyrolysis of Açai seeds (*Euterpe Oleracea*, Mart), activated with 2.0 M KOH solution, at 350, 400, and 450 °C, 1.0 atmosphere, in laboratory scale.

The FT-IR analysis of aqueous phase obtained by pyrolysis of Açai seeds (*Euterpe Oleracea*, Mart), activated with 2.0 M KOH solution, at 350, 400, and 450 °C, 1.0 atmosphere, in laboratory scale, illustrated in Figure 13. The FT-IR identified adsorption bands characteristic of chemical functions/chemical bonds of oxygenates, as shown in Table 5, confirming the presence of H<sub>2</sub>O, carboxylic acids, ketones, phenols, and alcohols, being according to similar analysis described elsewhere [57,58].

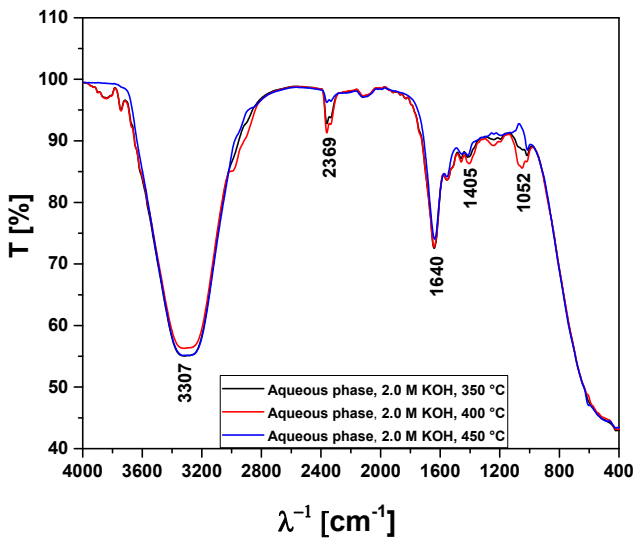


**Figure 13.** FT-IR analysis of aqueous phase obtained by pyrolysis of Açai seeds (*Euterpe Oleracea*, Mart), activated with 2.0 M KOH solution, at 350, 400, and 450 °C, 1.0 atmosphere, in laboratory scale.



**Table 5.** Absorption bonds and chemical functions identified by FT-IR analysis of aqueous phase obtained by pyrolysis of Açai seeds (*Euterpe Oleracea*, Mart), activated with 2.0 M KOH solution, at 350, 400, and 450 °C, 1.0 atmosphere, in laboratory scale.

Absorption Bands	Chemical Functions/Chemical Bonds
3400-3200 cm <sup>-1</sup>	-OH, hydrogen bond of alcohols and H <sub>2</sub> O.
2369 cm <sup>-1</sup>	<sub>ass</sub> -CO <sub>2</sub> , axial asymmetric deformation of CO <sub>2</sub> .
1648-1636 cm <sup>-1</sup>	C=C-C, C=C-C ring-related stretching associated to phenols.
1052 cm <sup>-1</sup>	C-O-C, C-O, C-H, C-O-C bond of esters, C-O bonds, and C-H bonds of benzene rings.

4.2.2. Process conditions, mass balances, and yields of reaction products by pyrolysis of activated Açai seeds (*Euterpe Oleracea*, Mart.) with HCl

The process parameters, mass balances, yields of reaction products (liquids, solids, H<sub>2</sub>O, and gas), and acidity of bio-oils by pyrolysis of activated Açai seeds at 350, 400, and 450 °C, 1.0 atm, activated with 2.0 M HCl, using a borosilicate glass reactor, in laboratory scale, are shown in Table 6.

**Table 6.** Process parameters, mass balances, yields of reaction products (liquids, solids, H<sub>2</sub>O, and gas), and acidity of bio-oils by pyrolysis of Açai seeds (*Euterpe Oleracea*, Mart), activated with 2.0 M HCl solution, at 350, 400, and 450 °C, 1.0 atmosphere, using a borosilicate glass reactor, in laboratory scale.

Process Parameters.	2.0 M HCl		
	350 °C	400 °C	450 °C
Mass of Açai seeds (g)	42.100	40.480	40.433
Cracking time (min)	72	72	72.0
Yield of Bio-oil (wt.%)	<b>3.37</b>	<b>2.84</b>	<b>2.13</b>
Yield of H <sub>2</sub> O (wt.%)	31.19	32.85	22.91
Yield of Hydro-char (wt.%)	47.53	35.08	37.32
Yield of Gas (wt.%)	17.91	29.22	37.64
Acidity (mg KOH/g)	127.1	128.9	218.5

The yields of bio-oil varied between 3.37 and 2.13% (wt.), decreasing with increasing pyrolysis temperature, showing that activation of Açai seeds with 2.0 M HCl do not favor the thermo-chemical transformation of biomass into bio-oil, compared to the chemical activation with 2.0 M KOH, illustrated in Table 2. This is according to Wang *et al.* [62], who investigated systematically the effect of acid (H<sub>2</sub>SO<sub>4</sub>) and basic (NaOH) pretreatment by pyrolysis of corn cob at 500 °C on the yield of reaction products [solid, liquid (bio-oil + aqueous phase), and gas] and chemical composition of liquid phase, showing that pretreatment of corn cob with NaOH for constant mass ratio (corn cob-to-acid/alkali) favors the liquid phase yields, compared to the pretreatment with H<sub>2</sub>SO<sub>4</sub>. In addition, Wang *et al.* [62], identified the presence of carboxylic acids (acetic acid), ketones (butanone), alcohol (methanol), furfural and aromatic hydrocarbon (benzene) in bio-oil by pyrolysis of alkali (NaOH) treated corn cob, while no aromatic hydrocarbon was identified in bio-oil by pyrolysis of acid (H<sub>2</sub>SO<sub>4</sub>) treated corn cob, being the major identified compounds, acetic acid, furfural, benzofuran, levoglucosan, and guaiacol [62]. The GC-MS analysis of bio-oil produced by pyrolysis of Açai seeds at 350, 400, and 450 °C, 1.0 atmosphere, with 2.0 M HCl, in laboratory scale, has not identified the presence of hydrocarbons, only oxygenates (carboxylic acids, alcohols, ketones, phenols, furans), as shown in Table 7, proving that pre-treatment of biomass with HCl before pyrolysis did not favor the formation of hydrocarbons, being according to the results of Wang *et al.* [62]. The results for the chemical composition of bio-oils in Table 7 are according to Bru *et. al.* [63], who investigated the main organic compounds in bio-oils obtained by pyrolysis of oak wood, showing that pyrolysis of acid washed oak wood produced bio-oil without hydrocarbons, that is, an acid pre-treatment of oak wood did not favor the formation of hydrocarbons [63]. The chemical functions, sum of peak areas, CAS numbers, and retention times of compounds identified in bio-oil and aqueous phase by GC-MS

analysis after pyrolysis of Açai seeds (*Euterpe Oleracea*, Mart), activated with 2.0 M HCl solution, at 350, 400, and 450 °C, 1.0 atmosphere, in laboratory scale, are illustrated in Supplementary Tables S7–S12.

**Table 7.** Chemical composition of major compounds (carboxylic acids, phenols) and oxygenates (alcohols, ketones, aldehydes, etc.) of bio-oil obtained by pyrolysis of Açai seeds (*Euterpe Oleracea*, Mart), activated with 2.0 M HCl solution, at 350, 400, and 450 °C, 1.0 atmosphere, in laboratory scale, identified by GC-MS.

Chemical Composition C <sub>i</sub> (area.%)	2.0 M HCl		
	350 °C	400 °C	450 °C
Carboxylic Acids	53.056	43.540	61.175
Phenols	35.945	32.700	26.682
Oxygenates (alcohols, aldehydes, ketones, cresols)	10.999	23.860	12.143
$\sum_i^n C_i$	100.00	100.00	100.00

Figure 14 and shows the FT-IR analysis of bio-oils produced by GC-MS analysis after pyrolysis of Açai seeds (*Euterpe Oleracea*, Mart), activated with 2.0 M HCl solution, at 350, 400, and 450 °C, 1.0 atmosphere, in laboratory scale. The FT-IR identified adsorption bands characteristic of chemical functions/chemical bonds of oxygenates, confirming the presence of alcohols, H<sub>2</sub>O, carboxylic acids, ketones, and benzene ring probably associated to furans in Figure 14, being according to similar analysis described elsewhere [11,31–34,57,58]. The FT-IR analysis of aqueous phase obtained by GC-MS analysis after pyrolysis of Açai seeds (*Euterpe Oleracea*, Mart), activated with 2.0 M HCl solution, at 350, 400, and 450 °C, 1.0 atmosphere, in laboratory scale, shown in Figure 15. The FT-IR identified adsorption bands characteristic of chemical functions/chemical bonds of oxygenates, confirming the presence of alcohols, H<sub>2</sub>O, carboxylic acids, and phenols, being according to similar analysis described elsewhere [11,31–34,57,58].

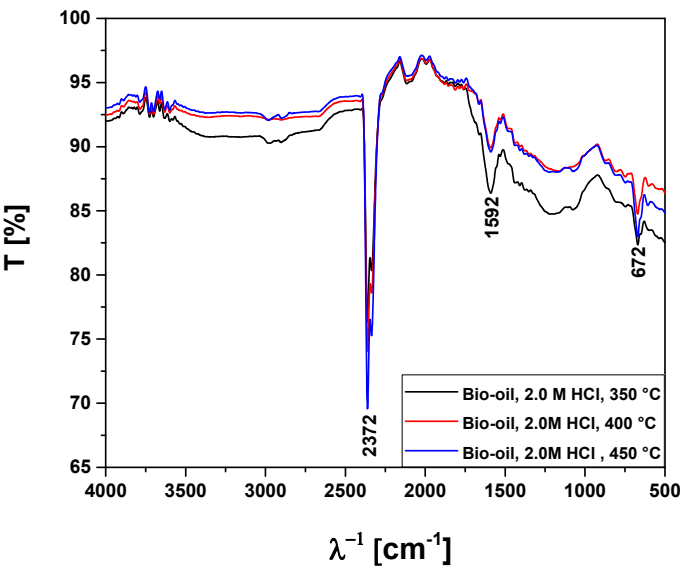


**Figure 14.** FT-IR analysis of bio-oils obtained by pyrolysis of Açai seeds (*Euterpe Oleracea*, Mart), activated with 2.0 M HCl solution, at 350, 400, and 450 °C, 1.0 atmosphere, in laboratory scale.

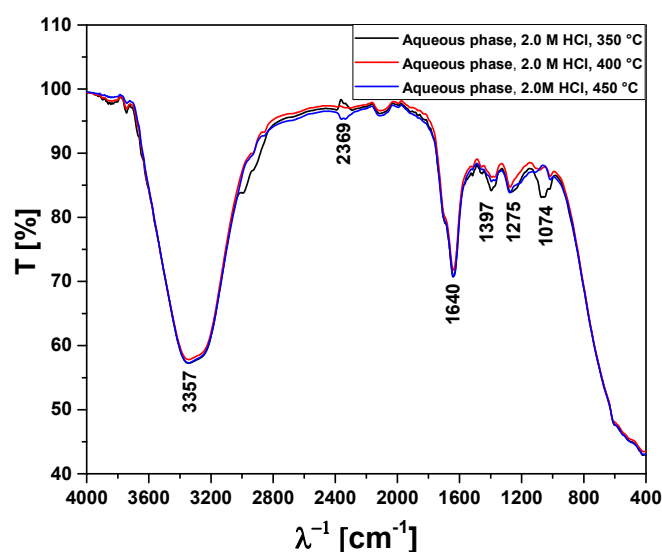


**Figure 15.** FT-IR analysis of aqueous phase obtained by pyrolysis of Açai seeds (*Euterpe Oleracea*, Mart), activated with 2.0 M HCl solution, at 350, 400, and 450 °C, 1.0 atmosphere, in laboratory scale.

## 5. Conclusions

XRD analysis of biochar produced by pyrolysis of Açai seeds at 350, 400, and 450 °C, 1.0 atmosphere, with 2.0 M KOH, in laboratory scale, shows the presence of Kalicinite ( $\text{KHCO}_3$ ), the dominant crystalline phase in biochar.

The yields of bio-oil by pyrolysis of activated Açai seeds at 350, 400, and 450 °C, 1.0 atm, activated with 2.0 M KOH, in laboratory scale, show a smooth increase with temperature, being correlated with a first order exponential decay model. In addition, by increasing the temperature, the concentrations of acyclic saturated/unsaturated hydrocarbons and heterocyclic hydrocarbons in bio-oil increase, while that of oxygenates (cresols, phenols, and ketones) decreases with increasing temperature, showing that higher pyrolysis temperatures favors the formation of hydrocarbons and disfavor the formation of oxygenates [57], as proved by a sharp decrease on the acidity of bio-oil, from 257.6 to 12.3 (mgKOH/g), due to a drastic decrease on the concentration of oxygenates.

The composition of aqueous phase produced by pyrolysis of activated Açai seeds at 350, 400, and 450 °C, 1.0 atm, activated with 2.0 M KOH, in laboratory scale, is according to similar studies reported in the literature [57–59], being identified the presence of carboxylic acids, ketones, alcohols, phenols, among other compounds. The acidity of aqueous phase decreases sharply with temperature, as the concentration of ketones in the aqueous phase decreases.

The yields of bio-oil by pyrolysis of activated Açai seeds at 350, 400, and 450 °C, 1.0 atm, activated with 2.0 M HCl, in laboratory scale, decrease with increasing temperature, showing that activation of Açai seeds with 2.0 M HCl do not favor the thermo-chemical transformation of biomass into bio-oil. In addition, it has not been identified the presence of hydrocarbons in bio-oil, only oxygenates, proving that acid (HCl) pre-treatment of Açai seeds did not enhance the yield of bio-oil nor favors the formation of hydrocarbons in bio-oil.

**Supplementary Materials:** The following are available. Table S1: Classes of compounds, summation of peak areas, CAS number, and retention times of chemical compounds identified by CG-MS in bio-oil by pyrolysis of Açai seeds (*Euterpe Oleracea*, Mart), activated with 2.0 M KOH solution, at 350 °C, 1.0 atmosphere, in laboratory scale. Table S2: Classes of compounds, summation of peak areas, CAS number, and retention times of chemical compounds identified by CG-MS in bio-oil by pyrolysis of Açai seeds (*Euterpe Oleracea*, Mart), activated with 2.0 M KOH solution, at 400 °C, 1.0 atmosphere, in laboratory scale. Table S3: Classes of compounds, summation of peak areas, CAS number, and retention times of chemical compounds identified by CG-MS in bio-oil by pyrolysis of Açai seeds (*Euterpe Oleracea*, Mart), activated with 2.0 M KOH solution, at 450 °C, 1.0 atmosphere,

in laboratory scale. Table S4: Classes of compounds, summation of peak areas, CAS number, and retention times of chemical compounds identified by CG-MS in aqueous phase by pyrolysis of Açaí seeds (*Euterpe Oleracea*, Mart), activated with 2.0 M KOH solution, at 350 °C, 1.0 atmosphere, in laboratory scale. Table S5: Classes of compounds, summation of peak areas, CAS number, and retention times of chemical compounds identified by CG-MS in aqueous phase by pyrolysis of Açaí seeds (*Euterpe Oleracea*, Mart), activated with 2.0 M KOH solution, at 400 °C, 1.0 atmosphere, in laboratory scale. Table S6: Classes of compounds, summation of peak areas, CAS number, and retention times of chemical compounds identified by CG-MS in aqueous phase by pyrolysis of Açaí seeds (*Euterpe Oleracea*, Mart), activated with 2.0 M KOH solution, at 450 °C, 1.0 atmosphere, in laboratory scale. Table S7: Classes of compounds, summation of peak areas, CAS number, and retention times of chemical compounds identified by CG-MS in bio-oil by pyrolysis of Açaí seeds (*Euterpe Oleracea*, Mart), activated with 2.0 M HCl solution, at 350 °C, 1.0 atmosphere, in laboratory scale. Table S8: Classes of compounds, summation of peak areas, CAS number, and retention times of chemical compounds identified by CG-MS in bio-oil by pyrolysis of Açaí seeds (*Euterpe Oleracea*, Mart), activated with 2.0 M HCl solution, at 400 °C, 1.0 atmosphere, in laboratory scale. Table S9: Classes of compounds, summation of peak areas, CAS number, and retention times of chemical compounds identified by CG-MS in bio-oil by pyrolysis of Açaí seeds (*Euterpe Oleracea*, Mart), activated with 2.0 M HCl solution, at 450 °C, 1.0 atmosphere, in laboratory scale. Table S10: Classes of compounds, summation of peak areas, CAS number, and retention times of chemical compounds identified by CG-MS in aqueous phase by pyrolysis of Açaí seeds (*Euterpe Oleracea*, Mart), activated with 2.0 M HCl solution, at 350 °C, 1.0 atmosphere, in laboratory scale. Table S11: Classes of compounds, summation of peak areas, CAS number, and retention times of chemical compounds identified by CG-MS in aqueous phase by pyrolysis of Açaí seeds (*Euterpe Oleracea*, Mart), activated with 2.0 M HCl solution, at 400 °C, 1.0 atmosphere, in laboratory scale. Table S12: Classes of compounds, summation of peak areas, CAS number, and retention times of chemical compounds identified by CG-MS in aqueous phase by pyrolysis of Açaí seeds (*Euterpe Oleracea*, Mart), activated with 2.0 M HCl solution, at 450 °C, 1.0 atmosphere, in laboratory scale.

**Author Contributions:** The individual contributions of all the co-authors are provided as follows: G.D.V. contributed with formal analysis and writing original draft preparation, investigation and methodology, F.P.V. contributed with formal analysis and writing original draft preparation, investigation and methodology, S.J.B. contributed with formal analysis and writing original draft preparation, K.C.A.B. contributed with investigation and methodology, L.H.H.G. contributed with chemical analysis, M.C.S. contributed with chemical analysis and methodology, L.P.B. contributed with formal analysis, investigation and methodology, W.P.F. contributed with physicochemical analysis and methodology, L.G.S.M. contributed with chemical analysis, N.M.M. contributed with formal analysis, investigation and methodology, D.A.R.d.C. contributed with investigation and methodology, S.D.J. contributed with resources, chemical analysis, L.E.P.B. contributed with resources, chemical analysis, and N.T.M. contributed with supervision, conceptualization, and data curation. All authors have read and agreed to the published version of the manuscript.

**Funding:** This research received no external funding.

**Institutional Review Board Statement:** Not applicable.

**Informed Consent Statement:** Not applicable.

**Acknowledgments:** I would like to acknowledge and dedicate this research in memory to Hélio da Silva Almeida, he used to work at the Faculty of Sanitary and Environmental Engineering/UFPa and passed away on 13 March 2021. His contagious joy, dedication, intelligence, honesty, seriousness, and kindness will always be remembered in our hearts.

**Conflicts of Interest:** The authors declare no conflict of interest.

## References

1. Andrezza de Melo Barbosa, Viviane Siqueira Magalhães Rebelo, Lucieta Guerreiro Martorano, Virginia Mansanares Giacon. Caracterização de partículas de açaí visando seu potencial uso na construção civil. revista Matéria, v.24, n.3, 2019, ISSN 1517-7076 artigo e-12435
2. Felipe Fernando da Costa Tavares, Marcos Danilo Costa de Almeida, João Antonio Pessoa da Silva, Ludmila Leite Araújo, Nilo Sérgio Medeiros Cardozo and Ruth Marlene Campomanes Santana. Thermal treatment of açaí (*Euterpe oleracea*) fiber for composite reinforcement. *Polímeros*, 30(1), e2020003, 2020, <https://doi.org/10.1590/0104-1428.09819>



3. D.R. Pompeu, E.M. Silva, H. Rogez. Optimisation of the solvent extraction of phenolic antioxidants from fruits of *Euterpe oleracea* using Response Surface Methodology. *Bioresource Technology* 100 (2009) 6076–6082, <https://doi.org/10.1016/j.biortech.2009.03.083>
4. Marcelo Morita Lindolfo, Gilson Sérgio Bastos de Matos, Wendel Valter da Silveira Pereira, Antonio Rodrigues Fernandes. Productivity and nutrition of fertigated açai palms according to boron fertilization. *Rev. Bras. Frutic., Jaboticabal*, 2020, v. 42, n. 2: (e-601)
5. Michael Heinrich, Tasleem Dhanji, Ivan Casselman. Açai (*Euterpe oleracea* Mart.)—A phytochemical and phar-macological assessment of the species' health claims. *Phytochemistry Letters* 4 (2011) 10–21
6. Sara Sabbe, Wim Verbeke, Rosires Deliza, Virginia Matta, Patrick Van Damme. Effect of a health claim and personal characteristics on consumer acceptance of fruit juices with different concentrations of açai (*Euterpe oleracea* Mart.). *Appetite* 53 (2009) 84–92
7. DAVID DEL POZO-INSFRAN, SUSAN S. PERCIVAL, AND STEPHEN T. TALCOTT. Açai (*Euterpe oleracea* Mart.) Polyphenolics in Their Glycoside and Aglycone Forms Induce Apoptosis of HL-60 Leukemia Cells. *J. Agric. Food Chem.* 2006, 54, 1222–1229
8. D. A. R. de Castro; H. J. da Silva Ribeiro; C. C. Ferreira; L. H. H. Guerreiro; M. de Andrade Cordeiro; A. M. Pereira; W. G. dos Santos; F. B. de Carvalho; J. O. C. Silva Jr.; R. Lopes e Oliveira; M. C. Santos; S. Duvoisin Jr; L. E. P. Borges; N. T. Machado. Fractional Distillation of Bio-Oil Produced by Pyrolysis of Açai (*Euterpe oleracea*) Seeds. Fractionation, Editor Hassan Al-Haj Ibrahim: Fractionation, Intechopen ISBN: 978-1-78984-965-3, DOI: 10.5772/intechopen.79546
9. Lauro Henrique Hamoy Guerreiro, Ana Cláudia Fonseca Baia, Fernanda Paula da Costa Assunção, Gabriel de Oliveira Rodrigues, Rafael Lopes e Oliveira, Sergio Duvoisin Junior, Anderson Mathias Pereira, Erika Milene Pinto de Sousa, Nélío Teixeira Machado, Douglas Alberto Rocha de Castro and Marcelo Costa Santos. Investigation of the Adsorption Process of Biochar Açai (*Euterpea olerácea* Mart.) Seeds Produced by Pyrolysis. *Energies* 2022, 15, 6234. <https://doi.org/10.3390/en15176234>
10. Bufalino, L.; Guimaraes, A.A.; de Silva, B.M.; de Souza, R.L.F.; de Melo, I.C.N.A.; de Oliveira, D.N.P.S.; Trugilho, P.F. Local variability of yield and physical properties of açai waste and improvement of its energetic attributes by separation of lignocellulosic fibers and seeds. *J. Renew. Sustain. Energy* 2018, 10, 053102
11. Douglas Alberto Rocha de Castro, Haroldo Jorge da Silva Ribeiro, Lauro Henrique Hamoy Guerreiro, Lucas Pinto Bernar, Sami Jonatan Bremer, Marcelo Costa Santo, Hélio da Silva Almeida, Sergio Duvoisin, Jr., Luiz Eduardo Pizarro Borges and Nélío Teixeira Machado. Production of Fuel-Like Fractions by Fractional Distillation of Bio-Oil from Açai (*Euterpe oleracea* Mart.) Seeds Pyrolysis. *Energies* 2021, 14, 3713. <https://doi.org/10.3390/en14133713>
12. Conceição de Maria Sales da Silva, Douglas Alberto Rocha de Castro, Marcelo Costa Santos, Hélio da Silva Almeida, Maja Schultze, Ulf Lüder, Thomas Hoffmann and Nélío Teixeira Machado. Process Analysis of Main Organic Compounds Dissolved in Aqueous Phase by Hydrothermal Processing of Açai (*Euterpe oleraceae*, Mart.) Seeds: Influence of Process Temperature, Biomass-to-Water Ratio, and Production Scales. *Energies* 2021, 14, 5608. <https://doi.org/10.3390/en14185608>
13. Anna Cristina Pinheiro de Lima, Dandara Leal Ribeiro Bastos, Mariella Alzamora Camarena, Elba Pinto Silva Bom, Magali Christe Cammarota, Ricardo Sposina Sobral Teixeira, Melissa Limoeiro Estrada Gutarra. Physicochemical characterization of residual biomass (seed and fiber) from açai (*Euterpe oleracea*) processing and assessment of the potential for energy production and bioproducts. *Biomass Conv. Bioref.* (2021) 11:925–935
14. Fassinou Wanignon Ferdinand, Laurent Van de Steene, Koua Kamenan Blaise, Toure Siaka. Prediction of pyrolysis oils higher heating value with gas chromatography–mass spectrometry. *Fuel* 96 (2012) 141–145
15. Lucas Pinto Bernar, Caio Campos Ferreira, Augusto Fernando de Freitas Costa, Haroldo Jorge da Silva Ribeiro, Wenderson Gomes dos Santos, Lia Martins Pereira, Anderson Mathias Pereira, Nathalia Lobato Moraes, Fernanda Paula da Costa Assunção, Sílvio Alex Pereira da Mota, Douglas Alberto Rocha de Castro, Marcelo Costa Santos, Neyson Martins Mendonça, Sergio Duvoisin, Jr., Luiz Eduardo Pizarro Borges and Nélío Teixeira Machado. Catalytic Upgrading of Residual Fat Pyrolysis Vapors over Activated Carbon Pellets into Hydrocarbons-like Fuels in a Two-Stage Reactor: Analysis of Hydrocarbons Composition and Physical-Chemistry Properties. *Energies* 2022, 15, 4587. <https://doi.org/10.3390/en15134587>
16. Caio Campos Ferreira, Lucas Pinto Bernar, Augusto Fernando de Freitas Costa, Haroldo Jorge da Silva Ribeiro, Marcelo Costa Santos, Nathalia Lobato Moraes, Yasmin Santos Costa, Ana Cláudia Fonseca Baia,

- Neyson Martins Mendonça, Sílvia Alex Pereira da Mota, Fernanda Paula da Costa Assunção, Douglas Alberto Rocha de Castro, Carlos Castro Vieira Quaresma, Sergio Duvoisin, Jr., Luiz Eduardo Pizarro Borges and Nélvio Teixeira Machado. Improving Fuel Properties and Hydrocarbon Content from Residual Fat Pyrolysis Vapors over Activated Red Mud Pellets in Two-Stage Reactor: Optimization of Reaction Time and Catalyst Content. *Energies* 2022, 15, 5595. <https://doi.org/10.3390/en15155595>
17. M.K. Sato, H.V. de Lima, A.N. Costa, S. Rodrigues, A.J.S. Pedroso, C.M.B. de Freitas Maia. Biochar from Acai agroindustry waste: study of pyrolysis conditions. *Waste Manag.*, 96 (2019), pp. 158-167
  18. Michel Keisuke Sato, Herdjanía Veras de Lima, Aline Noronha Costa, Sueli Rodrigues, Sacha J. Mooney, Michèle Clarke, Augusto José Silva Pedroso, Claudia Maria Branco de Freitas Maia. Biochar as a sustainable alternative to acai waste disposal in Amazon, Brazil. *Process Safety and Environmental Protection* 139 (2020) 36–46
  19. Leandro Rodriguez Ortiz, Erick Torres, Daniela Zalazar, Huili Zhang, Rosa Rodriguez, German Mazza. Influence of pyrolysis temperature and bio-waste composition on biochar characteristics. *Renewable Energy* 155 (2020) 837e847
  20. Leandro S. Queiroz, Luiz K.C. de Souza, Kelly Taise C. Thomaz, Erika Tallyta Leite Lima, Geraldo N. da Rocha Filho, Luis Adriano S. do Nascimento, Luiza H. de Oliveira Pires, Kelson do Carmo Freitas Faial, Carlos E.F. da Costa. Activated carbon obtained from amazonian biomass tailings (acai seed): Modification, characterization, and use for removal of metal ions from water. *Journal of Environmental Management* 270 (2020) 110868
  21. T.S. Pessôa, L.E. de Lima Ferreira, M.P. da Silva, L.M. Pereira Neto, B.F. do Nascimento, T.J.M. Fraga, E.F. Jaguaribe, J.V. Cavalcanti, M.A. da Motta Sobrinho. Açai waste benefiting by gasification process and its employment in the treatment of synthetic and raw textile wastewater. *J. Clean. Prod.*, 240 (2019), p. 118047
  22. Danilo Gualberto Zavarize. Insights on preparation and characteristics of KOH-doped carbons derived from an abundant agroindustrial waste in Brazil: Amazon açai berry seeds. *Bioresource Technology Reports* 13 (2021) 100611
  23. De Souza, L.K.C., Gonçalves, A.A.S., Queiroz, L.S., Chaar, J.S., da Rocha Filho, G.N., da Costa, C.E.F., 2020a. Utilization of acai stone biomass for the sustainable production of nanoporous carbon for CO<sub>2</sub> capture. *SM&T*, e00168. <https://doi.org/10.1016/j.susmat.2020.e00168>
  24. De Souza, T.N.V., Vieira, M.G.A., da Silva, M.G.C., Brasil, D. do S.B., de Carvalho, S.M.L., 2019. H<sub>3</sub>PO<sub>4</sub>-activated carbons produced from açai stones and Brazil nut shells: removal of basic blue 26 dye from aqueous solutions by adsorption. *Environmental Science and Pollution Research*, <https://doi.org/10.1007/s11356-019-04215-0>
  25. Araujo, R.O., Chaar, J. da S., Queiroz, L.S., da Rocha Filho, G.N., da Costa, C.E.F., da Silva, G.C.T., Landers, R., Costa, M.J.F., Gonçalves, A.A.S., de Souza, L.K.C., 2019. Low temperature sulfonation of acai stone biomass derived carbons as acid catalysts for esterification reactions. *Energy Convers. Manag.* 196, 821–830. <https://doi.org/10.1016/j.enconman.2019.06.059>
  26. De Souza, T.N.V., de Carvalho, S.M.L., Vieira, M.G.A., da Silva, M.G.C., Brasil, D. do S.B., 2018. Adsorption of basic dyes onto activated carbon: experimental and theoretical investigation of chemical reactivity of basic dyes using DFT-based descriptors. *Appl.Surf. Sci.* 448, 662–670. <https://doi.org/10.1016/j.apsusc.2018.04.087>
  27. Do Nascimento, B.F., de Araujo, C.M.B., do Nascimento, A.C., da Silva, F.L.H., de Melo, D.J.N., Jaguaribe, E.F., Lima Cavalcanti, J.V.F., da Motta Sobrinho, M.A., 2020. Detoxification of sisal bagasse hydrolysate using activated carbon produced from the gasification of açai waste. *J. Hazard. Mater.* 124494 <https://doi.org/10.1016/j.jhazmat.2020.124494>
  28. Ribeiro, L.A. de S., Thim, G.P., Alvarez-Mendez, M.O., dos Reis Coutinho, A., de Moraes, N.P., Rodrigues, L.A., 2018. Preparation, characterization, and application of low-cost açai seed-based activated carbon for phenol adsorption. *Int. J. Environ. Res.* 12, 755–764. <https://doi.org/10.1007/s41742-018-0128-5>
  29. De Souza, L.K.C., Martins, J.C., Oliveira, D.P., Ferreira, C.S., Gonçalves, A.A.S., Araujo, R.O., da Silva Chaar, J., Costa, M.J.F., Sampaio, D.V., Passos, R.R., Pocrifka, L.A., 2020b. Hierarchical porous carbon derived from acai seed bio-waste for supercapacitor electrode materials. *J. Mater. Sci. Mater. Electron.* 31, 12148–12157. <https://doi.org/10.1007/s10854-020-03761-5>
  30. de Andrade Cordeiro, M.; de Almeida, O.; de Castro, D.A.R.; da Silva Ribeiro, H.J.; Machado, N.T. Produção de Etanol através da Hidrólise Enzimática do Caroço de Açai (*Euterpe oleracea*, Mart.). *Rev. Bras. Energ. Renov.* 2019, 8, 122–152

31. H. da Silva Almeida, O.A. Corrêa, J.G. Eid, H.J. Ribeiro, D.A.R. de Castro, M.S. Pereira, L.M. Pereira, A. de Andrade Mâncio, M.C. Santos, J.A. da Silva Souza, Luiz E.P. Borges, N.M. Mendonça, N.T. Machado. Production of biofuels by thermal catalytic cracking of scum from grease traps in pilot scale. *Journal of Analytical and Applied Pyrolysis* 118 (2016) 20–33
32. H. da Silva Almeida, O.A. Corrêa, J.G. Eid, H.J. Ribeiro, D.A.R. de Castro, M.S. Pereira, L.M. Pereira, A. de Andrade Mâncio, M.C. Santos, S.A.P. da Mota, J.A. da Silva Souza, Luiz E.P. Borges, N.M. Mendonça, N.T. Machado. Performance of thermochemical conversion of fat, oils, and grease into kerosene-like hydrocarbons in different production scales. *Journal of Analytical and Applied Pyrolysis* 120 (2016) 126–143
33. H. da Silva Almeida, O.A. Corrêa, C.C. Ferreira, H.J. Ribeiro, D.A.R. de Castro, M.S. Pereira, A. de Andrade Mâncio, M.C. Santos, S.A.P. da Mota, J.A. da Silva Souza, Luiz E.P. Borges, N.M. Mendonça, N.T. Machado. Diesel-like hydrocarbon fuels by catalytic cracking of fat, oils, and grease (FOG) from grease traps. *Journal of the Energy Institute* 90 (2017) 337-354
34. S.A.P. da Mota, A.A. Mancio, D.E.L. Lhamas, D.H. de Abreu, M.S. da Silva, W.G. dos Santos, D.A.R. de Castro, R.M. de Oliveira, M.E. Araújo, Luiz E.P. Borges, N.T. Machado. Production of green diesel by thermal catalytic cracking of crude palm oil (*Elaeis guineensis* Jacq) in a pilot plant. *Journal of Analytical and Applied Pyrolysis* 110 (2014) 1–11
35. A.A. Mancio, S.A.P. da Mota, C.C. Ferreira, T.U.S. Carvalho, O.S. Neto, J.R. Zamian, M.E. Araújo, L.E.P. Borges, N.T. Machado. Separation and characterization of biofuels in the jet fuel and diesel fuel ranges by fractional distillation of organic liquid products. *Fuel* 215 (2018) 212–225
36. A.A. Mancio, K.M.B. da Costa, C.C. Ferreira, M.C. Santos, D.E.L. Lhamas, S.A.P. da Mota, R.A.C. Leão, R.O.M.A. de Souza, M.E. Araújo, L.E.P. Borges, N.T. Machado. Process analysis of physicochemical properties and chemical composition of organic liquid products obtained by thermochemical conversion of palm oil. *Journal of Analytical and Applied Pyrolysis* 123 (2017) 284–295
37. M.C. Santos, R.M. Lourenço, D.H. de Abreu, A.M. Pereira, D.A.R. de Castro, M.S. Pereira, H.S. Almeida, A.A. Mancio, D.E.L. Lhamas, S.A.P. da Mota, J.A. da Silva Souza, S.D. Júnior, M.E. Araújo, L.E.P. Borges, N.T. Machado. Gasoline-like hydrocarbons by catalytic cracking of soap phase residue of neutralization process of palm oil (*Elaeis guineensis* Jacq). *Journal of the Taiwan Institute of Chemical Engineers* 71 (2017) 106–119
38. C.C. Ferreira, E.C. Costa, D.A.R. de Castro, M.S. Pereira, A.A. Mancio, M.C. Santos, D.E.L. Lhamas, S.A.P. da Mota, A.C. Leão, S. Duvoisin, M.E. Araújo, Luiz E.P. Borges, N.T. Machado. Deacidification of organic liquid products by fractional distillation in laboratory and pilot scales. *Journal of Analytical and Applied Pyrolysis*, 127 (2017) 468-489, <https://doi.org/10.1016/j.jaap.2017.06.016>
39. B. Manoj, A.G. Kunjomana. Study of Stacking Structure of Amorphous Carbon by X-Ray Diffraction Technique. *Int. J. Electrochem. Sci.*, 7 (2012) 3127-3134
40. Nattaporn Prakongep, Robert J. Gilkes and Wanpen Wiriyakitnatekul. Agronomic benefits of durian shell biochar. *J. Met. Mater. Miner.* 24(1)2014, <https://doi.org/10.14456/jmmm.2014.2>
41. Jeong Han Lee, Young Lok Cha, Yong-Mook Kang, and Kwang Chul Roh. Study on the reaction mechanism of the potassium bicarbonate alkali activation process in black liquor. *APL Mater.* 10, 101105 (2022); <https://doi.org/10.1063/5.0104772>
42. J. Díaz-Terán, D.M. Nevskaja, J.L.G. Fierro, A.J. López-Peinado, A. Jerez. Study of chemical activation process of a lignocellulosic material with KOH by XPS and XRD. *Microporous and Mesoporous Materials*, 60 (2003) 173-181, [https://doi.org/10.1016/S1387-1811\(03\)00338-X](https://doi.org/10.1016/S1387-1811(03)00338-X)
43. Alisson Caio Magalhães Serrão, Conceição Maria Sales Silva, Fernanda Paula da Costa Assunção, Haroldo Jorge da Silva Ribeiro, Marcelo Costa Santos, Hélio da Silva Almeida, Sergio Duvoisin Jr., Luiz Eduardo Pizarro Borges, Douglas Alberto Rocha de Castro, Nélito Teixeira Machado. Process analysis of pyrolysis of Açaí (*Euterpe Oleracea*, Mart) seeds: Influence of temperature on the yield of reaction products and physico-chemical properties of Bio-Oil. *Brazilian Journal of Development*, Curitiba, v.7, n.2, p.18200-18220feb. 2021, DOI:10.34117/bjdv7n2-453
44. Piyali Das, Anuradda Ganesh. Bio-oil from pyrolysis of cashew nutshell—a near fuel. *Biomass and Bioenergy*, Volume 25, Issue 1, July 2003, 113-117
45. M. Asadullah; M. A. Rahman; M. M. Ali; M. S. Rahman; M. A. Motin; M. B. Sultan; M. R. Alam. Production of bio-oil from fixed bed pyrolysis of bagasse. *Fuel* Volume 86, Issue 16, November 2007, 2514-2520

46. Zheng Ji-lu. Bio-oil from fast pyrolysis of rice husk: Yields and related properties and improvement of the pyrolysis system. *J. Anal. Appl. Pyrolysis* 80 (2007) 30–35
47. Mohamad Azri Sukiran, Chow Mee Chin, Nor Kartini Abu Bakar. Bio-oils from Pyrolysis of Oil Palm Empty Fruit Bunches. *American Journal of Applied Sciences* 6 (5): 869-875, 2009
48. Seon-Jin Kim, Su-Hwa Jung, Joo-Sik Kim. Fast pyrolysis of palm kernel shells: Influence of operation parameters on the bio-oil yield and the yield of phenol and phenolic compounds. *Bioresource Technology*, Volume 101, Issue 23, December 2010, 9294-930
49. Gaurav Kumar, Achyut K. Panda, R. K. Singh. Optimization of process for the production of bio-oil from eucalyptus wood. *J Fuel Chem Technol*, 2010, 38(2), 162-167
50. Hyeon Su Heo, Hyun Ju Park, Jong-In Dong, Sung Hoon Park, Seungdo Kim, Dong Jin Suh, Young-Woong Suh; Seung-Soo Kim, Young-Kwon Park. Fast pyrolysis of rice husk under different reaction conditions. *Journal of Industrial and Engineering Chemistry*, Volume 16, Issue 1, 25 January 2010, 27-31
51. John V. Ortega, Andrew M. Renehan, Matthew W. Liberatore, Andrew M. Herring. Physical and chemical characteristics of aging pyrolysis oils produced from hardwood and softwood feedstocks. *Journal of Analytical and Applied Pyrolysis*, Volume 91, Issue 1, May 2011, 190-198
52. Rajeev Sharma, Pratik N. Sheth. Thermo-Chemical Conversion of Jatropha Deoiled Cake: Pyrolysis vs. Gasification. *International Journal of Chemical Engineering and Applications*, Vol. 6, No. 5, October 2015
53. Chaturong Paenpong; Adisak Pattiya. Effect of pyrolysis and moving-bed granular filter temperatures on the yield and properties of bio-oil from fast pyrolysis of biomass. *Journal of Analytical and Applied Pyrolysis*, Volume 119, May 2016, 40-51
54. Rahul Garg, Neeru Anand, Dinesh Kumar. Pyrolysis of babool seeds (*Acacia nilotica*) in a fixed bed reactor and bio-oil characterization. *Renewable Energy*, Volume 96, Part A, October 2016, 167-171
55. Anil Kumar Varma; Prasenjit Mondal. Pyrolysis of sugarcane bagasse in semi batch reactor: Effects of process parameters on product yields and characterization of products. *Industrial Crops and Products* 95 (2017) 704–717
56. Jordy Lima de Sousa, Lauro Henrique Hamoy Guerreiro, Lucas Pinto Bernar, Haroldo Jorge da Silva Ribeiro, Rafael Lopes e Oliveira, Marcelo Costa Santos, H lio da Silva Almeida, Sergio Duvoisin Jr., Luiz Eduardo Pizarro Borges, Douglas Alberto Rocha de Castro, N lio Teixeira Machado. *Brazilian Journal of Development*, Curitiba , v.7, n.2, p. 15549-15565feb. 2021, DOI:10.34117/bjdv7n2-261
57. Kathryn M. George, Travis C. Ruthenburg, Jeremy Smith, Lu Yu, Qi Zhang, Cort Anastasio, Ann M. Dillner. FT-IR quantification of the carbonyl functional group in aqueous-phase secondary organic aerosol from phenols. *Atmospheric Environment* 100 (2015) 230e237
58. A. E. Atabani, O. K. Al-Rubaye. Valorization of spent coffee grounds for biodiesel production: blending with higher alcohols, FT-IR, TGA, DSC, and NMR characterizations. *Biomass Conv. Bioref.* (2022) 12:577–596
59. Suping Zhang, Yongjie Yan, Tingchen Li, Zhengwei Ren. Upgrading of liquid fuel from the pyrolysis of biomass. *Bioresource Technology*, 96 (2005) 545-550, <https://doi.org/10.1016/j.biortech.2004.06.015>
60. Cristian Torri, Daniele Fabbri. Biochar enables anaerobic digestion of aqueous phase from intermediate pyrolysis of biomass. *Bioresource Technology*, 172 (2014) 335-341, <https://doi.org/10.1016/j.biortech.2014.09.021>
61. Haoqin Zhou, Robert C. Brown, Zhiyou Wen. Anaerobic digestion of aqueous phase from pyrolysis of biomass: Reducing toxicity and improving microbial tolerance. *Bioresource Technology*, 292 (2019) 121976, <https://doi.org/10.1016/j.biortech.2019.121976>
62. Xinde Wang, Shuai Leng, Jiaqi Bai, Hu Zhou, Xing Zhong, Guilin Zhuang and Jianguo Wang. Role of pretreatment with acid and base on the distribution of the products obtained via lignocellulosic biomass pyrolysis. *RSC Adv.*, 2015, 5, 24984–24989
63. K. Bru, J. Blin, A. Julbe, G. Volle. Pyrolysis of metal impregnated biomass: An innovative catalytic way to produce gas fuel. *J. Anal. Appl. Pyrolysis* 78 (2007) 291–300

**Disclaimer/Publisher’s Note:** The statements, opinions and data contained in all publications are solely those of the individual author(s) and contributor(s) and not of MDPI and/or the editor(s). MDPI and/or the editor(s) disclaim responsibility for any injury to people or property resulting from any ideas, methods, instructions or products referred to in the content.